EUROPHYSICS LETTERS 1 October 1999

Europhys. Lett., **48** (1), pp. 22-28 (1999)

Optical transmission through strong scattering and highly polydisperse media

J. Gómez Rivas[1], R. Sprik[1], C. M. Soukoulis[2], K. Busch[3] and A. Lagendijk[1]

[1] *Van der Waals-Zeeman Instituut, Universiteit van Amsterdam Valckenierstraat 65, 1018 XE Amsterdam, The Netherlands*
[2] *Ames Laboratory and Department of Physics and Astronomy Iowa State University, Ames, Iowa 50011, USA*
[3] *Institute for Theory of Condensed Matter, Department of Physics University of Karlsruhe - P.O. Box 6980, 76128 Karlsruhe, Germany*

(received 21 December 1999; accepted in final form 3 August 1999)

PACS. 42.25Dd – Wave propagation in random media.
PACS. 78.30Ly – Disordered solids.

Abstract. – We present near infrared total transmission measurements through samples of randomly packed silicon powders. At different wavelengths we analyze in detail the scattering properties and the effects of residual absorption. The lowest value of kl_s, where k is the wave vector and l_s is the scattering mean free path, is 3.2. We also observe that kl_s is nearly constant over a wide wavelength range. This phenomenon is associated with the high polydispersity of the particles. We use the energy density coherent potential approximation to explain our measurements.

The analogy between the propagation of electron waves and classical waves has led to a revival in the research of the transport of light in disordered scattering systems [1]. The final goal of many of these studies has been to observe the optical analogue of Anderson localization in electronic systems [2]. Anderson localization refers to an inhibition of the wave propagation in disordered scattering systems due to interference. Localization is essentially a wave phenomenon and it should hold for all kinds of waves *i.e.* electrons, electromagnetic and acoustic waves [3]. For isotropic scatterers Anderson localization is established if $kl_s \leq 1$, where k is the wave vector in the medium and l_s is the scattering mean free path, or the average length that the wave propagates in between two elastic collisions. The transition between extended and localized states occurs when $kl_s \simeq 1$. This is known as the Ioffe-Regel criterion for localization [4]. To approach the Ioffe-Regel criterion, l_s can be reduced by using scatterers with a high refractive index, n, and a size such that the scattering cross-section is maximum. Experimental difficulties in realizing a random medium where the optical absorption is low enough and the light scattering is efficient enough to induce localization has been the reason why, for a long time, only microwave localization was realized [5]. In this experiment the absorption is large and, therefore, complicates the interpretation of the results. Recently, near

infrared localization in GaAs powders was observed [6]. Nevertheless, the validity of these measurements has been questioned by the possibility of absorption [6]. It is clear that new experiments must be carried out in very strong scattering media to distinguish between the effects of optical absorption and multiple scattering.

In this letter we present near infrared total transmission measurements through samples of randomly packed silicon powders with particle sizes of the order the wavelength, λ. Silicon is a semiconductor with the energy band gap at $\lambda_{\rm gap} = 1.1\ \mu$m. Therefore, the measurements were performed at wavelengths, $\lambda > \lambda_{\rm gap}$ to minimize optical absorption. The high refractive index of Si ($n \simeq 3.5$ in the near infrared) and the size of the Si particles constituting our samples make the light-matter coupling very strong. We have performed measurements at different wavelengths to systematically study the influence of the residual band gap absorption and the scattering properties of the system.

The transition between extended and localized states occurs when $kl_{\rm s} \simeq 1$. If $kl_{\rm s} \gg 1$, light propagates by performing a random walk. An enormous simplification in the description of the transport of light can thus be made by neglecting all interference effects, and the transport may be described by the diffusion equation [7]. As $kl_{\rm s}$ approaches the critical value, the diffusion approximation may still be used with a renormalized diffusion constant. In the localization regime the steady-state diffusion breaks down, which means that the diffusion constant vanished. Defining the transport mean free path, l, as the distance traveled by the light before its direction of propagation becomes randomized, isotropic scattering implies that l equals $l_{\rm s}$. If we consider a medium translationally invariant in the x and y directions, the three-dimensional diffusion equation reduces to the one-dimensional case in the non-translationally invariant direction, *i.e.* the z-direction. This is valid for slab-geometry samples in which the x and y dimensions are much larger than the z-dimension. Then, the energy density in the stationary state inside the sample, ρ, is given by

$$\frac{\partial^2 \rho}{\partial z^2} - \frac{\rho}{L_{\rm a}^2} = -\frac{1}{D} I_0 \delta(z - l)\ , \tag{1}$$

where $L_{\rm a}$ is the absorption length and D the diffusion constant. The diffusion constant is given by $D = v_{\rm e} l/3$, where $v_{\rm e}$ is the energy transport velocity in the medium. In eq. (1), the incoming energy flux at the boundary $z = 0$ has been replaced by a source of diffusive radiation of strength, I_0, equal to the incident flux and located at the plane $z = l$ [8]. Simulations have shown that eq. (1) is accurate to within about 1% for slabs sufficiently thick to be opaque [9].

The boundary conditions are determined considering that the diffuse fluxes going into the sample at $z = 0$ and L are due to a finite reflectivity at the boundaries [10]. The boundary conditions can be written as

$$\rho \mp z_{0_i} \frac{\partial \rho}{\partial z} = 0\,, \qquad i = \begin{cases} 1 \text{ if } z = 0 \text{ (front sample surface)}\,, \\ 2 \text{ if } z = L \text{ (back sample surface)}\,, \end{cases} \tag{2}$$

where z_{0_i} are given by $z_{0_i} = (2l/3)(1 + \overline{R_i})/(1 - \overline{R_i})$, and $\overline{R_i}$ are the polarization and angular averaged reflectivities of the boundaries. In the non-absorbing limit ($L_{\rm a} \to \infty$) eqs.(2) are equivalent to extrapolate ρ to 0 at a distance z_{0_i} outside the sample surface. Therefore z_{0_i} are called the extrapolation lengths. If $\overline{R_i} = 0$ the diffusion approximation gives $z_{0_i} = 2l/3$, very close to the extrapolation length of $0.7104l$ given by the Milne solution [7].

The experimentally determined quantities in our experiments are the total transmitted intensities. The total transmission, defined as the transmitted flux normalized by the incident

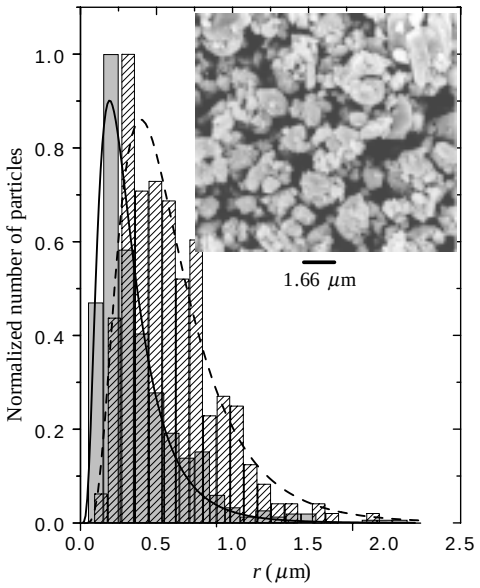

Fig. 1

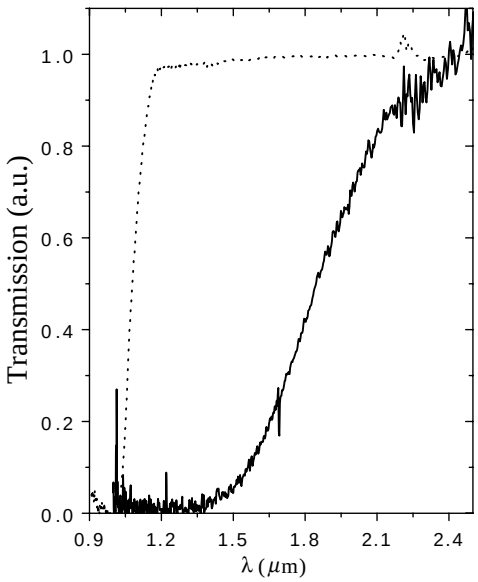

Fig. 2

Fig. 1. – Normalized histograms of the silicon particle radius considering all the particles as entities, independently of whether they are part of a cluster (solid bars), and considering the clusters as single particles (dashed bars). The solid and dotted lines are log-normal fits, from which the average particle radius are calculated. The inset is a scanning electron microscope photograph of the Si particles.

Fig. 2. – Total transmission spectra normalized to their maximum transmissions. Solid line: Total transmission spectrum of a layer of silicon powder of 57.8 μm thickness. Dotted line: Transmission spectrum of a piece of intrinsic silicon of 1 mm thickness.

flux, is given by [11]

$$T = \frac{-D(\nabla\rho)_{z=L}}{I_0} = \frac{\sinh(l/L_\mathrm{a}) + (z_{0_1}/L_\mathrm{a})\cosh(l/L_\mathrm{a})}{(1 + z_{0_1}z_{0_2}/L_\mathrm{a}^2)\sinh(L/L_\mathrm{a}) + (1/L_\mathrm{a})(z_{0_1} + z_{0_2})\cosh(L/L_\mathrm{a})} \,. \quad (3)$$

If $L_\mathrm{a} \gg L$, eq. (3) simplifies to

$$T = \frac{l + z_{0_1}}{L + z_{0_1} + z_{0_2}} \,, \quad (4)$$

and if $L_\mathrm{a} \ll L$, it simplifies to

$$T = \frac{2L_\mathrm{a}(l + z_{0_1})}{L_\mathrm{a}^2 + (z_{0_1} + z_{0_2})L_\mathrm{a} + z_{0_1}z_{0_2}} \exp[-L/L_\mathrm{a}] \,. \quad (5)$$

In our experiments we measure the total transmission through samples consisting of 99.999% pure Si particles. These powders are commercially available (Cerac S-1049) containing particles with sizes ranging from a few hundred nanometers to about 40 μm. To reduce the polydispersity of the powders we suspended them in spectroscopic chloroform and we let the Si particles sediment for 5 minutes. Only the particles that did not sediment were used in the experiments. The polydispersity of the resulting powder was evaluated from scanning electron microscope photographs like the one showed in the inset of fig. 1. As can be seen in the photograph, the particles tend to aggregate into clusters. This makes the definition of particle

radius difficult. We have evaluated the average particle radius with two different methods: a) considering all the particles as entities, independently of if they are part of a cluster, and b) considering the clusters as single particles. Defining the radius of a particle (or a cluster) as half the maximum distance between parallel tangents to the particle surface, we computed the radius of the particles. Figure 1 shows the normalized histograms of the particle radius. The histograms can be fitted with a log-normal function, $y = A\exp[-\ln^2(r/r_c)/2W^2]$. The fit to the histogram obtained with method a) gives $A = 0.90$, $r_c = 0.19$ μm, $W = 0.61$, and it is shown by the solid line in fig. 1, while method b) gives $A = 0.86$, $r_c = 0.44$ μm, $W = 0.55$, and it is shown by the dotted line in the same figure. This allows to calculate the average particle radius and its standard deviation: a) $r_a = 0.33 \pm 0.22$ μm, and b) $r_a = 0.69 \pm 0.41$ μm. The polydispersity defined as the ratio between the standard deviation and r_a in percentage, is of 67% and 59%, respectively. In other words, our samples are constituted by highly polydisperse scatterers.

We evaporated the chloroform and made slab geometry samples with the remaining powder on CaF_2 substrates with the form of a disk of 10 mm diameter. The thicknesses of the powder's layers were measured, with a resolution of 1 μm, with an optical microscope. We measured the thickness of each sample at different points within its central region to be sure that the powder layer was homogeneous. The resulting sample thicknesses are the average value of these measurements and they range from 5.9 ± 2 μm to 57.8 ± 2 μm.

The total transmissions were measured with a Fourier Transform Infrared Spectrometer (BioRad FTS-60A). A tungsten halogen lamp was the light source. Short wavelengths were optically filtered and an aperture of 2 mm diameter was placed in front of the sample to measure the transmission only through the region where the thickness was measured. The power of light incident on the sample was $\simeq 1$ mW. The diffusely transmitted light was collected with a $BaSO_4$-coated integrating sphere and detected with a PbSe photoconductive cell. Before and after measuring each sample, we measured the transmission through a clean CaF_2 substrate, which we used as reference to obtain the absolute value of the total transmission through the Si layer and to check the stability of the set-up. Figure 2 shows a total transmission spectrum of a sample of thickness $L = 57.8$ μm (solid line), and the transmission spectrum of a piece of intrinsic Si of 1 mm thickness (dotted line) for comparison. Both measurements have been normalized by their maximum transmissions.

By weighing the samples, we estimated the Si volume fraction to be $\phi \simeq 40\%$, which gives rise to a Maxwell-Garnet effective refractive index of the samples of $n_e \simeq 1.5$, nearly constant for wavelengths between 1.4 μm and 2.5 μm. With the value of n_e, the extrapolation lengths of the Si-air and Si-CaF_2 interfaces (z_{0_1} and z_{0_2}, respectively) can be calculated. Due to the size and irregular shape of the Si particles, we may assume that the scattering is isotropic. Then, since $l = l_s$, the values of the extrapolation lengths are estimated to be $z_{0_1} \simeq 2.42\, l_s$ and $z_{0_2} \simeq 0.78\, l_s$; these are taken as fixed parameters in eq. (3) and eq. (4). Figure 3 shows the total transmission as a function of the sample thickness for $\lambda = 2.5$ μm (squares) and $\lambda = 1.4$ μm (circles). The error bars are mainly due to intensity fluctuations of the source and to inhomogeneities in the sample thickness. The total transmission measurements can be fitted excellently by using classical diffusion theory as it is shown by the solid and dotted lines in fig. 3. The solid line in fig. 3 is a fit of eq. (4) to the $\lambda = 2.5$ μm measurements with $l = l_s = 0.83 \pm 0.08$ μm. At this wavelength $L_a \gg 57.8$ μm, thus absorption can be neglected. The dotted line is a fit of eq. (3) to the $\lambda = 1.4$ μm measurements with $l = l_s = 0.56 \pm 0.06$ μm and $L_a = 8.8 \pm 1$ μm.

The wavelength dependence of L_a is plotted in fig. 4. The increase of absorption for $\lambda < 2.0$ μm is due to strain in the Si lattice structure. The presence of strain gives rise to a deformation of the potential which smears the valence and conduction bands. This results in an

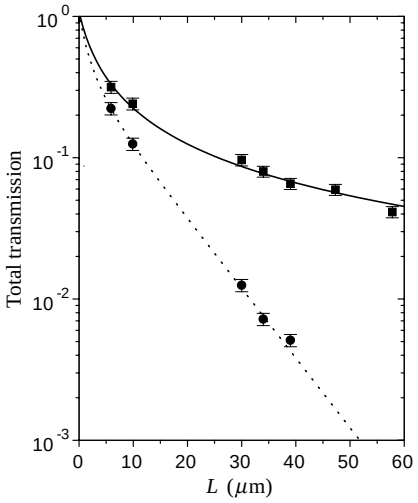

Fig. 3

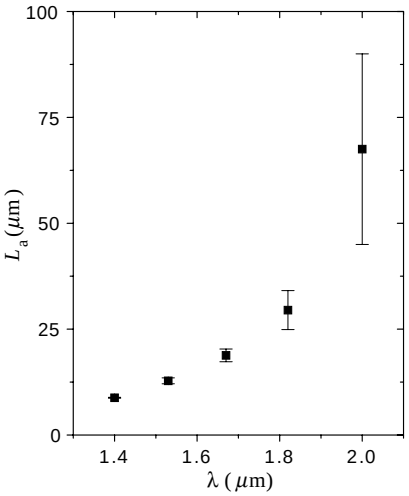

Fig. 4

Fig. 3. – Total transmission through silicon powders as a function of the sample thickness. The squares are the measurements for $\lambda = 2.5$ μm. The solid line is a fit using classical diffusion theory in a non-absorbing medium, eq. (4), with $z_{0_1} = 2.42\,l_s$, $z_{0_2} = 0.78\,l_s$ and $l_s = 0.83$ μm. The circles are the measurements for $\lambda = 1.4$ μm. At this wavelength absorption plays a role as can be seen from the fit using classical diffusion theory in an absorbing medium (dotted line), eq. (3), with $z_{0_1} = 2.42\,l_s$, $z_{0_2} = 0.78\,l_s$, $l_s = 0.56$ μm and $L_a = 8.8$ μm.

Fig. 4. – Absorption length in silicon powders *vs.* the wavelength.

extension to longer wavelengths of the semiconductor band gap which decreases considerably the absorption length at sub-band gap energies with respect to the strain-free material. We have confirmed the presence of strain in our Si with X-ray diffraction measurements.

In fig. 5 l_s is plotted as function of λ. It is remarkable that l_s does not depend strongly on λ, which can be attributed to the high polydispersity of the Si particles. We have used the Energy Density Coherent Potential Approximation (EDCPA) [12,13] to calculate the transport properties in a random media composed of Si spheres ($\phi = 40\%$) with a size distribution given by a log-normal function ($A = 0.86$, $r_c = 0.44$ μm, $W = 0.55$). The solid line in fig. 5 is a convolution of the calculated l_s for the specific spheres sizes with the probability density function given above. As can be seen there is a good qualitative agreement between the measured and the calculated l_s. The quantitative difference can be attributed to several factors: In the EDCPA calculation the scatterers are spheres, which clearly is not the case in the Si samples. As pointed out before there is not an unambiguous way of measuring the particle radius due to the aggregation of particles, we find better agreement between theory and experiments when we consider the particle clusters as single scatterers. For comparison, we plot in fig. 5 (dotted line) the calculated l_s in a system composed of monodisperse Si spheres of radius 0.44 μm and 40% volume fraction.

Using l_s from the total transmission measurements, we can estimate the Ioffe-Regel parameter, $kl_s = 2\pi n_e l_s/\lambda$. In fig. 6 we have plotted the resulting values of kl_s as a function of λ. Due to the slow change of l_s with λ, kl_s remains nearly constant in the measured wavelength interval. The line in fig. 6 is the result when using l_s from the EDCPA calculation considering the polydispersity in the particle sizes. Although the values of kl_s are very close to the critical

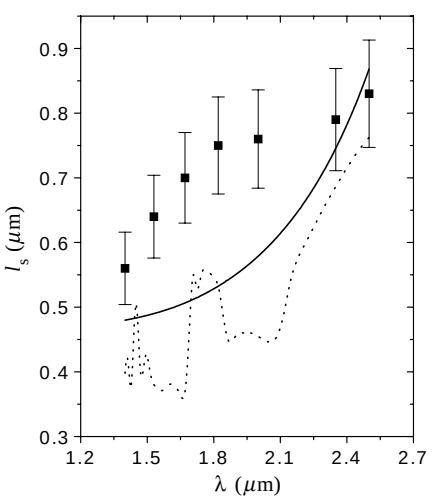

Fig. 5

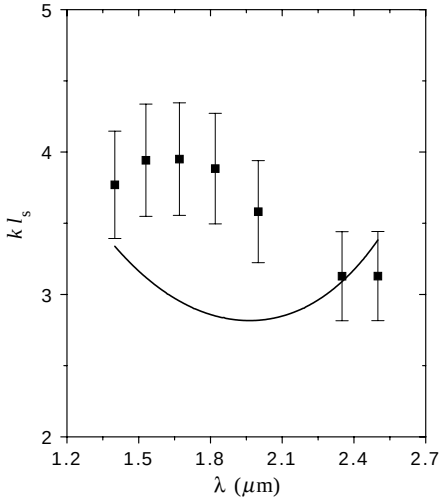

Fig. 6

Fig. 5. – Scattering mean free path, l_s, of light measured in silicon powders *vs.* the wavelength. The Si volume fraction has been estimated to be $\phi \simeq 40\%$. The solid line is a convolution of l_s, calculated with the energy density coherent potential approximation, for the specific spheres sizes with the probability density function given by the dotted line in fig. 1 and $\phi = 40\%$. The dotted line is l_s calculated for a monodisperse system of Si spheres (radius=0.44 μm) and the same volume fraction.

Fig. 6. – Values of kl_s in silicon powders *vs.* the wavelength. The line is kl_s of a polydispere system of Si spheres calculated with the Energy Density Coherent Potential Approximation.

value of $kl_s \simeq 1$, we can, nonetheless, describe our results using classical diffusion theory. Wiersma *et al.* have reported the observation of Anderson localization of light in submicron GaAs powders [6]. The refractive indices of GaAs and Si are almost equal and the volume fraction and the size of the scatterers in the GaAs and Si samples are comparable. Therefore, the high values kl_s and, consequently, the apparent absence of Anderson localization in the GaAs samples is a surprising result that needs further theoretical attention. In ref. [12], Kirchner *et al.* using the EDCPA found that the values of kl_s for the inverse structure of air spheres in high dielectric materials is much lower that those for the direct structure of spheres of high dielectric material in air. A possible explanation for the lower value of kl_s in the GaAs samples could be a different connectivity of the particles. The shape of the GaAs particles [14] is not as spherical as the shape of the Si particles. Therefore the contact between neighboring particles could be better in the GaAs than in the Si samples. Then, the GaAs samples may be better represented by an inverse structure while for the Si samples a description in terms of a direct structure may be preferred.

In conclusion, we have studied the wavelength dependence of the scattering properties and the absorption in very strong scattering and highly polydisperse media. From total transmission measurements of light of wavelength between 1.4 μm and 2.5 μm through samples consisting of very polydisperse Si particles, we obtain the scattering mean free path, l_s, and the absorption length, L_a. The scattering mean free path depends weakly on the wavelength λ, giving rise to a nearly constant value of the Ioffe-Regel parameter kl_s for the range of λ we have considered. This phenomenon can be understood in terms of the high polydispersity of the Si particles. Our results can be fully described using classical diffusion theory. This is

remarkable because recently Anderson localization of light has been reported in a very similar scattering medium (gallium arsenide powders) [6]. A possible difference between the samples of ref. [6] and the Si samples used in this work could be the connectivity of the particles.

***

We acknowledge P. DE VRIES, R. H. J. KOP, F. J. P. SCHUURMANS, D. S. WIERSMA and W. L. VOS for fruitful discussions, H. P. SCHRIEMER for carefully reading this manuscript and W. TAKKENBERG for his assistance with the scanning electron microscope. JGR wants also to thank the European Commission for financial support through Grant No. ERBFMBICT971921.

REFERENCES

[1] SHENG P., *Introduction to Wave Scattering, Localization, and Mesoscopic Phenomena* (Academic Press, New York) 1995.

[2] ANDERSON P. W., *Phys. Rev.*, **109** (1958) 1492.

[3] JOHN S., *Phys. Rev. Lett.*, **53** (1984) 2169; ANDERSON P. W., *Philos. Mag. B*, **52** (1985) 505.

[4] IOFFE A. F. and REGEL A. R., *Prog. Semicond.*, **4** (1960) 237.

[5] GARCIA N. and GENACK A. Z., *Phys. Rev. Lett.*, **66** (1991) 1850.

[6] WIERSMA D. S., BARTOLINI P., LAGENDIJK A. and RIGHINI R., *Nature*, **390** (1997) 671; SCHEFFOLD F., LENKE R., TWEER R. and MARET G., *Nature*, **398** (1999) 206.

[7] ISHIMARU A., *Wave Propagation and Scattering in Random Media*, Vol. **1** and Vol. **2** (Academic Press, New York) 1978.

[8] AKKERMANS E., WOLF P. E. and MAYNARD R., *Phys. Rev. Lett.*, **56** (1986) 1471.

[9] DURIAN D. J., *Phys. Rev. E*, **50** (1994) 857.

[10] LAGENDIJK A., VREEKER R. and DE VRIES P., *Phys. Lett. A*, **136** (1989) 81; ZHU J. X., PINE D. J. and WEITZ D. A., *Phys Rev. A*, **44** (1991) 3948.

[11] GARCIA N., GENACK A. Z. and LISYANSKY A. A., *Phys. Rev. B*, **46** (1992) 14475.

[12] BUSCH K. and SOUKOULIS C. M., *Phys. Rev. Lett.*, **75** (1995) 3442; KIRCHNER A., BUSCH K. and SOUKOULIS C. M., *Phys. Rev. B*, **57** (1998) 277.

[13] SOUKOULIS C. M., DATTA S. and ECONOMOU E. N., *Phys. Rev. B*, **49** (1994) 3800.

[14] We have milled GaAs as described in ref. [6] and scanning electron microscope photographs of the powder show that the GaAs particles have edges and facets.